# Structural Analysis of Spent Fuel Dry Storage Facility Against Aircraft Collision

Tae-Yong Kim[a], Jae Min Sim[a] and Yoon-Suk Chang [a*]
[a]*Dept. of Nuclear Engineering, Kyung Hee University, 1732 Deokyoungdae-ro, Yongin, Kyunggi, 446-701, Korea*
[*]*Corresponding author: yschang@khu.ac.kr*

## 1. Introduction

Spent fuel contains long half-life fission products and a lot of radioactive nuclei releasing high-temperature radiation for a long time. As wet storage facilities in nuclear power plants are saturated, the application of dry storage has increased since the 1990s, and it is now being used in 10 countries [1].

As the danger of aircraft terrorism appears, the necessity of safety evaluation against aircraft collision has been raised in nuclear facilities. In many previous studies, safety assessment subjects were confined to reactor containment buildings. As the necessity for dry storage management has been emphasized, evaluation of dry storage facilities was demanded.

In this study, structural integrity evaluation was conducted for Modular Air-Cooled Storage (MACSTOR) which is a kind of dry storage facility. The aircraft was modeled as Smoothed-Particle Hydrodynamics (SPH), and the Riera method based on NEI 07-13 [2] was applied to validate the model. Subsequently, postulated dry storage building and the validated aircraft were used for analysis. Structural analyses were performed using the commercial program LS-DYNA [3]. As a typical result, displacements of MACSTOR taking into account concrete damage were derived.

## 2. Analysis methods and conditions

### *2.1 Riera method*

In order to verify the aircraft model before the impact analysis, theoretical impact force-time history was derived based on Eq. (1), which is presented in NEI 07-13 [2].

$$F_m(t) = P_c[x(t)] + \alpha\mu[x(t)]v_m(t)^2 \qquad (1)$$

where $P_c[x(t)]$ is the crushing force. $\mu[x(t)]$ represents the mass of the aircraft per unit length [4, 5], and α is the effective mass coefficient. In this paper, crushing force was set to 10 % of the total impact force, and $\alpha$ was conservatively assumed to be 1.0 without mass attenuation. $v_m(t)$ was fixed to 150 m/s during the collision.

### *2.2 Aircraft model*

#### *2.2.1 SPH method*

SPH has advantage for large deformation analysis such as aircraft collision. Unlike Finite Elements Method (FEM), SPH is a particle based modeling method. Fig. 1. shows the constructed aircraft using the SPH method. The particle approximation of a function is Eq. (2) [3].

$$\prod h f(x) = \int f(y)W(x-y,h)dy \qquad (2)$$

where $W$ is the kernel function, and $h$ is the smoothing length, $d$ is number of dimensions. The analysis was carried out by colliding the aircraft with a speed of 150 m/s vertical to the rigid wall.

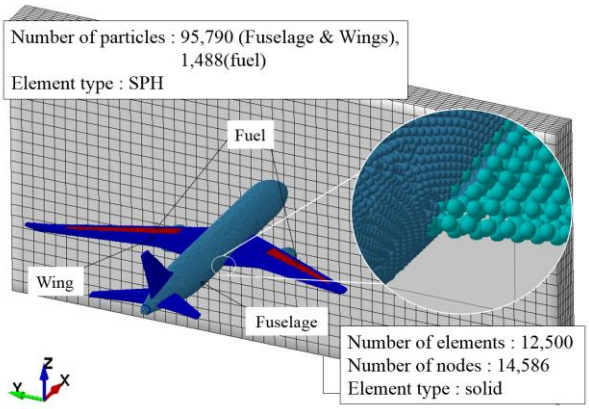


Fig. 1. Aircraft and rigid wall

#### *2.2.2 Material properties*

Fig. 2 depicts mass distribution of the aircraft based on the x-axis direction, and the sum of the masses is 204,100 kg. Especially, the mass of the aircraft is concentrated on the aircraft wings, fuel, and fuselage.

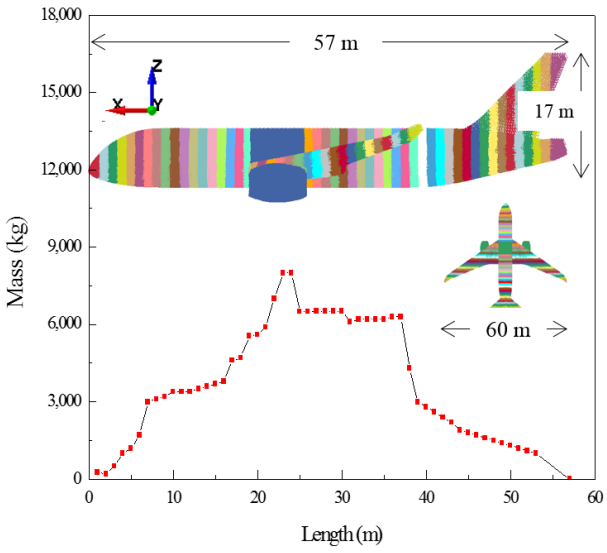


Fig. 2. Aircraft mass distribution

The aircraft fuselage and wings were constructed by the model of Mat Plastic Kinematic/Mat 003 summarized in Table 1 [5]. Mat Null / Mat 009 and Grüneisen Equation Of State (EOS) [6] based on Eq. (3) were adopted to reflect fluid properties of the fuel.

$$P = \frac{c_0^2 \rho_0 \eta}{(1-s\eta)^2}\left(1 - \frac{\Gamma_0 \eta}{2}\right) + \Gamma_0 \rho_0 E_m \qquad (3)$$

Table I: Material properties of aircraft [5]

| | |
|---|---|
| Density (kg/m$^3$), $\rho$ | 2,700 |
| Young's modulus (GPa), $E$ | 70 |
| Tangent modulus (GPa), $E_t$ | 10 |
| Yield strength (MPa), $\sigma_{dy}$ | 300 |
| Poisson ratio, $\nu$ | 0.3 |
| Hardening parameter | 0.5 |

Table II: Material properties of fuel [6]

| | |
|---|---|
| Density (kg/m$^3$), $\rho$ | 1,000 |
| Dynamic viscosity (N·s/m$^2$), $\mu$ | 100 |
| Speed of sound (m/s), $c_0$ | 1,560 |
| Fitting constants, $s$ | 2.0 |
| Grüneisen constant, $\Gamma_0$ | 1.1 |

### *2.3 Verification*

Fig. 3 represents comparison of impact force-time histories derived from Eq. (1) and the analysis. Analytical solution was filtered with 50 Hz and 200 Hz which is recommended by NEI 07-13 [2] to reduce the fluctuation. At 0.13 s the fuselage, wings, fuel collided with rigid wall at the same time, so the maximum value of impact force was generated.

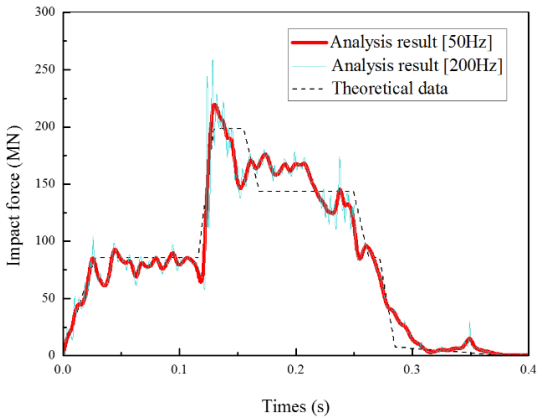


Fig. 3. Impact force-time histories

Fig. 4 is the impulse curve obtained by integrating the impact force curve over the time. Since oscillation of red one was lesser than blue one, the former one was adopted for the impulse-time history. The endpoints of analytical and theoretical data had a difference of 0.62 %. The analysis results obtained by the same procedure with validation of the aircraft with SPH model was confirmed through comparison with shell elements [7]. The impact force- and impulse- time histories depicted in Figs 3 and 4 were more consistent with those obtained from the previous study.

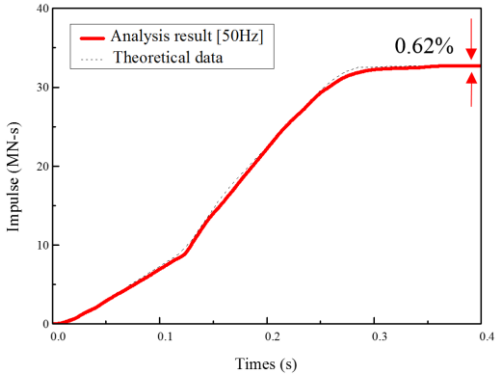


Fig. 4 Impulse-time history

## 3. Aircraft impact simulation on a MACSTOR

### *3.1 Analysis model*

Fig. 5 shows the FE model of MACSTOR and its mesh information as well as verified aircraft. Due to the lack of detail information, material properties of reinforced concrete were used from the previous study [7] and assumed to be elastic deformation without strain rate effect. To take into account the concrete material failure, the erosion criterion was set to 1.05 for CSCM (MAT 159) [8]. It means that the concrete elements are deleted when the damage exceeds 0.99 and the maximum principal strain exceeds 0.05 [8].

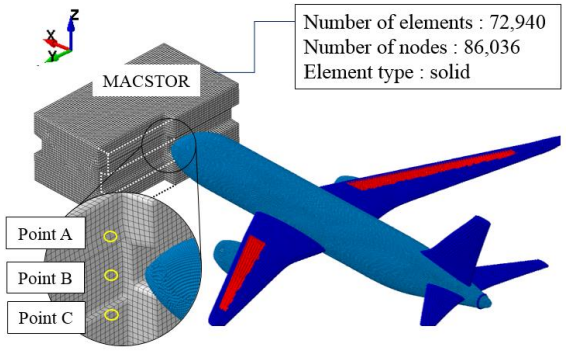


Fig. 5. FE model of MACSTOR and collision positions

### *3.2 Analysis conditions*

The initial velocity of the aircraft was given 150 m/s along the x-axis direction. The aircraft was designated as slave part and MACSTOR was defined as master part [3]. The * CONTACT-AUTOMATIC-NODES-TO-SURFACE option was used for contact between two parts. Also, the floor of the facility was completely fixed. The analysis time was set to 0.45 s. Points A, B and C represent three heights of spent nuclear storage in the central part of MACSTOR.

*3.3 Analysis Result*

Fig. 6 shows variation of displacements at the representative points shown in Fig. 5. Displacement of point C saturated to 100 mm after 0.4 s when the aircraft has completed the collision. The displacements of points A and B were 371 mm and 346 mm respectively at 4 s, and then increased continuously due to the influence of inertia. The displacement of A was higher than that of B at 0.45 s.

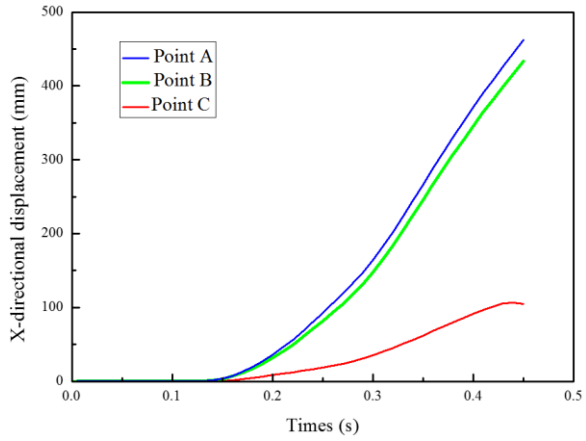


Fig. 6. Variation of displacements at 3 points

## 4. Conclusions

In this study, the structural integrity of the dry storage facility was evaluated by colliding the aircraft consisted by SPH model.

(1) In order to demonstrate the aircraft model, theoretical and analytical impact force-time histories were compared. As a result, the maximum values of the two histories had little differences, and end points of impulse-time histories matched within 0.62 %.

(2) From the impact analysis, the displacements at the bottom of MACSTOR converged after the collision of the aircraft. However, those of the top and middle increased continuously due to the inertia.

## ACKNOWLEDGMENTS

This work was supported by "Human Resources Program in Energy Technology" of the Korean Institute of Energy Technology Evaluation and Planning (KETEP), granted financial resource from the Ministry of Trade, Industry & Energy, Republic of Korea (No. 20184030202170)

## REFERENCES

[1] Y.S. Chang, J.H. Jung, "Introduction to Nuclear Fuel Management", Hans House, 2017.
[2] Nuclear Energy Institute (NEI 07-13), "Methodology for Performing Aircraft Impact Assessments for New Plat Designs", 2009.
[3] Livermore Software Technology Corporation, "LS-DYNA Keyword User's Manual 971", 2007.
[4] S. S. Shin, T. H. Park, "Analysis of containment building subjected to a large aircraft impact using a hydrocode", J. of the Korean Soc. of Civ. Eng. 31 5A, pp. 369-378, 2011.
[5] T. Zhang, H. Wu, Q. Fang and Z. M. Gong, "Influences of nuclear containment radius on the aircraft impact force based on riera function", Nucl. Eng. Des. 293, pp. 196-204, 2015.
[6] S. S. Shin, D. Hahm, T. H. Park, Shock vibration and damage responses of primary auxiliary buildings from aircraft impact, Nucl. Eng. Des. 310, pp. 57-68, 2016.
[7] J. M. Sim, Y. S. Chang, Y., "Structural integrity assessment of containment and interior components against postulated aircraft impact", Int. Workshop. Integr. Nucl. Compon, 2018.
[8] S. H. Kim, Y. S. Chang, Y. J. Cho and M. J. Jhung, "Modeling of Reinforced Concrete for Reactor Cavity Analysis under Energetic Steam Explosion Condition", Nucl. Eng. Tec.48, pp. 218-277, 2016.
[9] K. S. Lee, J. W. Jung and J. W. Hong, "Advanced aircraft analysis of an F-4 Phantom on a reinforced concrete building", Nucl. Eng. Des. 273, pp. 505-528, 2014.